Sampling waste printed circuit boards: Achieving the right combination between particle size and sample mass to measure metal content

Solène Touze, Sylvain Guignot, Agathe Hubau, Nicolas Devau, Simon Chapron

1 **Title:** Sampling waste printed circuit boards: achieving the right combination between

2 particle size and sample mass to measure metal content

3 **Key words**: waste PCB, sampling, characterisation, metals, recycling, urban mining

4 **Corresponding author:** Solène Touzé – s.touze@brgm.fr

5 **Authors:** S. TOUZE[1], S. GUIGNOT[1], A. HUBAU[1], N. DEVAU[1], S. CHAPRON[1]

6 1-BRGM, 3 av. Claude Guillemin, 45060 Orléans, France

7

Highlights:

- Ni, Co, Fe, Cu, Pb and Zn content and of associated RSD in waste PCBs were determined
- Effects of sample mass, grain size, and number of replicates were evaluated
- Nugget effect was identified in Ni and Co distributions
- Margins of error in metal content were determined by statistical bootstrap tool
- This study provides a decision-making tool to find the best WPCB preparation method

Abstract

The current worldwide expansion of waste PCB (WPCB) deposits represents both a pressing environmental issue and an economic opportunity, fostering the development of numerous recycling processes across the world. An important input for designing such processes is the metallic content of WPCBs, which is assayed by grinding and leaching samples taken from the stack of WPCBs to be recycled. The content values come with substantial uncertainties, arising mainly from the uneven distribution of the metals within the structure of WPCBs.

This study aims to quantify the effects on these uncertainties of the particle size, the mass of the sample digested and the number of digestion replicates. It focused on the abundance of six metals in WPCBs: Cu, Fe, Zn, Pb and Ni, and also Co, which is a critical element for the EU. A batch of 485 kg of WPCBs was put through several shredding and splitting steps to produce three fractions: one shredded to 2 mm, and two ground to 750 μm and 200 μm. From each sample, 16 samples of 0.5 g, 2 g or 5 g were digested in hot aqua regia. Bootstrapping of the results allowed the error around the mean content to be estimated, for each metal and for all the experimental conditions. Considering the largest sample masses and three replicated digestions, the uncertainties for Zn (resp. Ni) were reduced from 35 % to 10 % (resp. from 70 % to 10 %) when the particle size was reduced from 2 mm to 200 μm.

1. Introduction

Recycling of Waste Printed Circuit Boards (WPCBs) from Waste Electrical and Electronic Equipment (WEEE) is a major challenge in sustainable resource management. The quantities involved are significant: in 2019, the production of WPCBs amounted to 23 ktons in France and more than 170 ktons in the European Union (EU), according to the European urban mine database (WEB 1). Since 2000, numerous recycling chains have been set up to treat this type of waste and to recover some of the metals from WPCBs, and are now well established and operational (Ghosh et al., 2015; Rocchetti et al., 2018). In the EU, the state-of-the art technologies mostly involve pre-processing (shredding/physical separation of some elements), and end-processing to extract and refine the metals by pyrometallurgical (smelting or pyrolysis) and hydrometallurgical operations (Ning et al, 2017). Smelting operations are conducted in large facilities originally built to produce metals from copper sulphide concentrates, and as such, the design of the pre-processing and refining steps must take into account not only the complexity of the WPCB materials to be processed, but also the operational capacities and limitations of the smelters. Consequently, the range of metals that are potentially recoverable by applying current recycling options is still limited, as are the rates of recovery. Base metals (such as copper and nickel) and precious metals (gold, platinum and palladium) can be partially recovered, while other elements (such as Sb and Ta) are still left as waste. Furthermore, in order to maximize their operating profits, industrial recyclers primarily target so-called rich WPCBs, i.e. those with the highest concentration of precious metals, to the detriment of WPCBs with lower concentrations, so that these are largely unaddressed. This context has prompted intense R&D efforts over the last two decades or so (recent reviews in Ning et al., 2017; Awasthi et al., 2018) to develop alternative treatments that are better suited to the diversity of WPCBs and their complex

compositions. Obviously, knowledge of the metal composition of WPCBs is crucial 1) to quantify metal flows 2) to quantify losses of metals in recycling chains 3) to explore new processes and markets 4) to adapt recycling processes to changing trends in waste production and 5) to track potentially polluting metals.

To draw a parallel with the design of a metallurgical process for ore beneficiation, the more care is taken in preparing and *sampling* the stack and performing efficient *chemical analyses*, or *assaying*, the more accurate the composition of a given stack of waste PCBs will be.

Sampling aims to obtain a sample which is *representative* of the whole stack, i.e. which contains all the constituents and in exactly the same proportion in which they occur in the stack. This is to reduce the risk of misclassifications of materials, which affects decision-making and the cost analysis process. In the ore mining and beneficiation field, the conventional recommendations to enhance the representativeness of samples taken from a pile of materials are to sample fractions of finer particle sizes and to use larger sampling masses, in order to improve the overall homogenization and to limit potential over/under-representation of certain elements (Gy, 1979). The larger the mass sizes, the closer the sample will be to the mean composition of the stack. Likewise, the finer the particle sizes, the more homogeneous the sample is likely to be. Samples are prepared by applying comminution techniques (including shredding and grinding), and splitting steps. However, WPCBs are characterized by high spatial heterogeneities in their composition and in the physical properties of their constituent materials, which tends to challenge homogenization efforts. In terms of composition, WPCB materials consist of several alternating layers of copper and fibreglass-reinforced polymer resins, with various components (resistors, capacitors, transistors and integrated circuits) soldered onto one of the outermost surfaces.

In terms of chemical composition, up to 60 different elements go into the manufacture of microprocessors and circuit boards, usually in tiny and dispersive quantities, in combinations that are not found in nature (Bloodworth, 2014), and closely intermingled with phenolic moulding or epoxy resins often reinforced by fibreglass. The multiple applications and corresponding equipment embedded in printed circuit boards translate into many different chemical compositions of WPCBs. The current general consensus on composition is approximately 60 $(\%)_{wt}$ of non-metallic elements, divided into glass and ceramics (30%) and plastics (30%), and 40 $(\%)_{wt}$ of metals, which include base metals (Cu, Fe, Al, Sn, Pb, Zn, Ni), precious metals (Pd, Au, Ag), and other valuable metals such as In, Co and Ta (Kaya, 2016). Metals can exist as discrete particles (large or small "nuggets"), as a surface layer and as inclusions (alloy). This complex composition, and especially the fact that there are several orders of magnitude between the most and least concentrated metals in a given circuit board is the first major challenge met when trying to obtain representative samples. This is because a highly concentrated metal is likely to be more homogeneously distributed among the samples produced after a size reduction and splitting process, so that the variability of the metal content among samples will be low. Conversely, the sub-sample mass and its particle size will have much more influence on the distribution of an element with a low metal content, and the probability of obtaining differences in the analyses of replicates will be higher (Gy, 1979).

One way to improve homogenization is to work with samples with finer grain sizes, but this brings in a second challenge: the very different mechanical properties of the various parts of the WPCBs, in terms of malleability and ductility, and which react differently to the grinding conditions applied. What is then often observed is stiffer and brittle parts being more easily broken into smaller fragments than ductile ones, as well as limitations on the smallest size

that the whole sample can be ground down to. However, this step is often performed only to a partial extent in studies in the literature, in the sense that plastics (Arshadi and Mousavi, 2015; Hossain et al., 2018) or specific components such as the hard fraction (Li et al, 2012; Priya and Hait, 2018a; Korf et al., 2019; Holgersson et al., 2018) are removed before the size reduction steps. In other studies, the sample is not wholly reduced below a target size; instead, undersize sieved fractions are selected, with no further consideration given to the oversize parts (Ogunniyi et al., 2009; Zhao et al., 2017; Korf et al., 2019). This is often ascribed to the flexible or ductile parts elongating into flakes larger than the sieve apertures, and therefore remaining in the milling equipment chamber (Hubau et al., 2019; Otsuki et al., 2019). One additional point is that grinding WPCBs to fine particles may generate significant losses of valuable elements as dust and through heating (Yamane et al., 2011). In practice, a quantitative reduction of a whole WPCB to a size below 250 μm at most seems difficult to achieve by conventional means, i.e., without resorting to cryogenic mills for example (Ernst et al., 2003; Wienold et al., 2011; Zhou et al., 2016). This constitutes a limitation on the homogenization of the samples when the aim is to characterize the metal content of the whole WPCB and not only of specific fractions produced from them.

The two challenges, complex composition and the different mechanical properties of constituent WPCB parts, are sometimes intertwined. Owing to some metals being at once in the form of surface layers and quite ductile, “nuggets” of very pure metal can be found in every size class in the middlings obtained after preparation by milling. Such cases then compromise the quality of homogenization, and thereby challenge the subsequent sampling procedure, in that the samples may not accurately reflect the distribution of these nuggets, resulting for example in wide variations in elements observed in various sub-samples taken from the same sample.

Sampling procedures that take the above-mentioned specificities of WPCBs into account do not seem to be described in the literature. Besides the specific standards applied to solid fuels (DIN 51701-2) or electro-technical products (IEC 62321-2), which are only partial and rarely accessible, information is available on the “in-house” industrial practices applied by the main WPCB recyclers in Europe. Umicore has published its own sampling process in operation for electronic scrap in its Hoboken plant. The chemical analysis is run with samples with particles ranging from 100 µm to 300 µm, but there is no information on how the WPCBs are milled to these sizes (Hagelüken, 2006). It is not possible to learn from their procedure because the Hoboken sampling and assaying unit was changed for reasons of efficiency between 2011 and 2013 and no information was published on the new processes (UMICORE, 2012). Other industrial sampling procedures use smelting or calcination before the analysis stage (Laubertova et al., 2019).

With regard to *chemical analysis* of ground WPCB samples, several studies recommend the use of aqua regia digestion for metal characterization (Ogunniyi et al., 2009; Mičková et al., 2018; Andrade et al., 2019). As regards reference material to validate the analysis results, there was no standard reference material available for WEEE and WPCBs at the time of our study (Mičková et al., 2018). Since then, Andrade et al. (2019) have developed a standard WPCB material for metals analysis, but the associated uncertainty remains at a high level for the metals of interest here (14.08 ± 5.67% mass Cu, 3.92 ± 2.05% mass Fe, 0.42 ± 0.15% mass Ni, 1.19 ± 0.20% mass Pb, and 1.36 ± 0.71% mass Zn). BAM has also proposed a reference material from ashed WPCBs that were melted with pyrite (BAM M505a, Bundesanstalt für Materialforschung und prüfung, Berlin), but the final matrix is notably different from shredded WPCBs, due in particular to the absence of plastics. Finally, Priya and Hait (2018b) use a polyethylene reference material in their study but the range of metal

concentrations is significantly different to that currently found in WPCBs (100 ppm of Fe in the material vs. around 10% Fe in WPCBs). The characterization of base metal concentrations in WPCBs would benefit from the development of new certified reference materials.

The scientific literature contains some data on the effects of the particle size and sub-sample mass, along with the number of digestion replicates, on the accuracy of a given chemical analysis, particularly for WPCB samples with a coarse particle size. Wienold et al. (2011) studied the influence of 5 digestion processes, using different sub-sample masses for analysis (0.1 to 5 g) and 4 particle sizes (120 µm, 250 µm, 500 µm and 1500 µm), on the precision and reproducibility of elemental analysis (Cu, Pb, Cd, Hg) (Wienold et al., 2011). In Wienold's analysis for Cu, Pb and Cd, to achieve a relative standard deviation (RSD) of less than 20%, samples had to be ground to a particle size of < 500 µm. The influence of the sample mass and the digestion protocol was also investigated by Ernst et al. (2003) using samples with a -250 µm particle size. The masses were variable (from 0.5 to 10 g) for the hot aqua regia digestion protocol in quadruplicate. In Ernst's analysis, the RSD is below 20% for all metals for a sub-sample mass of 0.5 g and below 8% for 10 g(Ernst et al., 2003). Andrade et al. (2019) argue the reverse, with a standard deviation that increases, for most metals, as the sample mass increases.

Based on these previous studies, the significance of each of these variables (particle size, mass of the sample used for the digestion protocol, along with the number of digestion replicates) is still difficult to assess. Moreover, none of these studies evaluates the influence of the combination of all these three parameters simultaneously on the uncertainties as to

174 the metal content, and none of them quantifies the error associated with numerous
175 repetitions.

176 Given these considerations, the purpose of the present study was therefore to investigate
177 the effects of the three parameters on the data distribution and to calculate the associated
178 margin of error for metal content found in WPCBs. The metals were chosen among those
179 found in the highest concentrations in WPCBs: Cu, with concentrations around 14 $(\%)_{wt}$, Fe
180 3$(\%)_{wt}$, Pb 2.5$(\%)_{wt}$, Ni 0.4$(\%)_{wt}$ and Zn 0.2$(\%)_{wt}$ (Bizzo et al. 2014). The study also addresses
181 the case of Co, as a sparsely distributed element in WPCBs and a critical material for the EU.
182 The sample masses considered are 0.5, 2 and 5 g, and span an order of magnitude that
183 includes most of the masses used in the vast majority of studies dealing with the
184 characterization of WPCBs. Three samples, obtained after initial coarse shredding to 10 mm
185 followed by a careful sampling procedure, were further shredded until they could pass
186 through mill apertures of 2 mm, 750 µm and 200 µm respectively. These sizes correspond to
187 various degrees of liberation of the metal parts, according to the literature (Otsuki et al.,
188 2020; Bacher et al, 2017, Guo et al., 2011). For a given set of mass and particle size, 16
189 digestions were performed following the same protocol. This substantial number of
190 repetitions is a compromise between technical feasibility and a sufficient number for
191 deriving statistics. This number should make it possible to quantify the uncertainties as to
192 metal content and to identify the maximum sources of error (preparation bias and nugget
193 effect for example). Statistical processing of all the data and bootstrapping of the results
194 were performed to estimate the uncertainties as to metal concentrations, as depicted by the
195 spread of the confidence interval around the mean content, or margin of error, for each
196 experimental condition and each metal. The aim here was to assess and highlight the
197 importance of the particle size, the sample mass and the number of digestion replicates

when considering the development of an efficient WPCB sampling and wet assaying methodology. Our study also aims to provide information on choosing the right combination of these three parameters to obtain a given uncertainty as to the metal content.

2. Materials and methods

2.1. Sample preparation

The WPCBs used for this study were taken from the Small Waste Electrical and Electronic Equipment (sWEEE) category, which comprises audio and video appliances, toys, personal care products and culinary equipment among others. Approximately 500 kg of waste was provided by “Envie 2E Midi-Pyrénées”, a waste recovery company operating in France. Materials with harmful environmental impacts, such as batteries, were disassembled, as well as aluminium heat sinks.

The entire sample (485kg) was first shredded with an industrial cutting mill without any bottom sieve (Bohmier Maschinen GmbH Material) to a particle size of less than 30 mm. The sample was subsequently quartered with a rotary divider. One quarter of the sample (122kg) was then shredded with the industrial cutting mill with a bottom sieve with 10 mm perforations, to a particle size of less than 10 mm. The < 10 mm sample was divided with a riffle splitter to obtain sub-sample masses of 4 kg. Three 4kg samples were used for the tests: i) 2 mm sample: this 4kg sample was shredded in a lab knife mill (Retsch SM2000 with tungsten carbide grinding tools) fitted with a bottom sieve with 2 mm perforations, ii) 750 µm sample: this 4 kg sample was shredded in the same lab knife mill fitted successively with bottom sieves of 2 mm, 1 mm and 750 µm and iii) 200 µm sample: this 4kg sample was shredded to 750 µm in the lab knife mill and sent to the Poittemille company (Bethune,

220 France) to be milled with a Universal grinder (FL1 Poittemille) using 200 µm ring holes.
221 Sample preparation is detailed in figure 1.

222 In the further shredding steps, the hammer rotation and the initial feed rates were kept
223 constant. The milling times were not fixed, but correspond to the minimum length of time
224 needed for at least 95% of the feed to pass through the sieve aperture. The unground
225 portion was added to the ground material to produce the same composition as the original
226 WPCB samples. After grinding, a riffle divider was used to obtain sub-samples of 5 g, 2 g and
227 0.5 g from the 4 kg samples.

228 The losses of material were less than 1 % in the procedure to obtain the 2 mm and 750 mm
229 samples. The losses associated with the size reduction from 750 µm to 200 µm are unknown.
230 The sampling methodology, with the yields and losses associated with each step, is detailed
231 in a previous article by Hubau (Hubau et al., 2019).

232 To determine the particle size distribution, samples of more than 290 g were suspended in
233 water and passed through vibrating sieves with square apertures of 4 mm, 2 mm, 1 mm, 800
234 µm, 400 µm, 200 µm, 100 µm, 63 µm and 20 µm. The size fractions were then dried at 40 °C.

235 2.2. Digestion procedure and analyses

236 All the WPCB samples were characterised by aqua regia digestion followed by chemical
237 analysis using Flame Atomic Absorption Spectrometry (FAAS). The samples were dissolved in
238 hot aqua regia (HNO_3:HCl 1:3) at reflux, in a vessel equipped with a condenser. The solid
239 /liquid ratio was 1:10 (weight/volume), and the contact time was about 2h. Each leaching
240 fraction was filtered over a 0.45 µm cellulose nitrate filter, and the leachate was diluted with
241 a solution of HNO_3 0.5 M. The concentrations of Fe, Cu, Zn, Pb, Ni and Co in the resulting
242 solutions were determined by Flame Atomic Absorption Spectrometry FAAS on a Varian

243 SpectrAA-300. Details on the digestion process are given in Hubau et al. (2019). All the
244 chemicals used were of analytical reagent grade.

245 2.3. Experimental programme

246 In order to understand the effects of sub-sample mass and particle size on the accuracy of
247 the metal content determination, 3 samples of different particle sizes (200 µm, 750 µm and
248 2 mm) and 3 different sub-sample masses for digestion (0.5 g, 2 g and 5 g) were studied.
249 Combining these two parameters produced nine different conditions. To be able to perform
250 statistical tests, it was decided to repeat each condition at least 16 times; each metal
251 content value represents one measurement of one digestion. The number of independent
252 digestions was respectively: for the 200 µm sample: 5g n=16, 2g n=16, 0.5g n=16; for the 750
253 µm sample: 5g n=24, 2g n=16, 0.5g n=16 and for the 2 mm sample: 5g n=24, 2g n=16, 0.5g
254 n=16. However, for the 0.5 g sample with a 750 µm particle size, one digestion vessel broke
255 during the digestion, so the number of repetitions considered is 15 for this condition.

256 2.4. Statistical analyses

257 For each metal, statistical analyses were performed to distinguish the gap between the
258 experimental mean value of the metal content from the “true” mean value, which would
259 represent the analysis of an infinite number of replicates. The 95% confidence interval was
260 used to quantify this gap. This interval refers to the range of values in which the “true” mean
261 value has a 95% chance of being. It thus depicts the uncertainty over the determination of
262 the metal content. In this study, the 95% confidence interval expressed relatively to the
263 corresponding mean value was called the margin of error (in percentage of the experimental
264 mean value).

For each metal, the normality and the homoscedasticity of the distribution of the metal concentrations for the nine associated treatments (combination of the 3 different particle sizes and the 3 different sub-sample masses) were tested using the Shapiro test (test to determine whether the distribution is normal) and the Bartlett test (test to determine whether the samples were from populations with equal variances), respectively. For some metals (Co, for instance), the measured values associated with some treatments did not follow a normal distribution, according to these tests. These results prevent the use of the classic parametric approach, based on the central limit theorem associated with the Student distribution, to calculate the population variance and draw inferences for the confidence interval. In order to overcome this limitation, an approach based on bootstrapping was used, which is not restricted to a specific type of probability distribution. In the bootstrap approach, the hypothesis is made that the measured data for each treatment and for each of the 6 metals are an empirical estimate of the probability distribution. For each treatment performed on the 6 metals, 25 metal content values were randomly selected in succession from the set of experimental data. Replacement was performed, i.e. the same experimental value could have been selected an infinite number of times. From these 25 values, a mean value was calculated. These random selections and mean value calculations were performed more than 10 000 times. From these 10 000 mean values, the 95% confidence interval around the mean value of the metal content was determined. The margin of error was then calculated, i.e. the confidence interval relatively to the experimental mean value. In order to assess the impact of the digestion replicates (n) on the estimation of statistical population properties, several bootstrap sampling sizes were tested (n=2, n=3, n=4, n=5, n=7, n=10, n=15, n=25). All the statistical tests were carried out using R-software 3.5.2 (R Core Team, 2019).

289 3. Results and discussion

290 3.1. Particle size distribution

291 The particle size distributions of the different samples are shown in figure 2. The d80 (i.e.
292 80% passing size) of the particle size distribution was equal to 150 µm, 750 µm and 1.8 mm
293 for the 200 µm, 750 µm and 2 mm samples respectively. For the 750 µm sample, 20% of the
294 mass was composed of particles larger than 750 µm because shredding was incomplete : for
295 each shredding, some particles did not pass through the bottom sieve of the mill. These
296 particles were added to the milled material to preserve the representativeness of the
297 samples and to ensure that the comparison of the metal content in the three samples would
298 not be distorted.

299 3.2. Estimation of potential biases arising from sample preparation and analysis

300 Despite the fact that no particles were removed during the shredding steps, the additional
301 grinding steps for 750 µm and 200 µm compared to 2 mm were liable to generate some
302 interference, including contamination due to the abrasion of mill material or preferential
303 metal losses (dust dispersion for example). One way of highlighting the influence of these
304 different sample preparations is to compare the mean values of the different conditions
305 (table 1). The mean values for metal content remained of the same order of magnitude with
306 no erratic points. Wienold et al. (2011) showed a similar trend for Pb content: the Pb content
307 analysis (digested sample mass of 2 g) of coarse samples (scrap and 1.5 mm) remained of the
308 same order of magnitude as for the finest samples (500 µm, 250 µm and 120 µm). If the
309 additional grinding steps had generated a bias, this bias would have affected the mean value
310 for each particle size sample differently. For example, if Pb was lost due to dust dissipation
311 during the additional grinding steps, we would systematically have less Pb in 200 µm than in
312 2 mm samples. For all metals, the minimum mean values were not systematically present in

one particle size sample, and likewise for the maximum mean values. This observation shows that there was no evident bias for Ni, Pb, Zn, Fe, Cu and Co mean contents in relation to the additional shredding step.

In order to verify the efficiency of the digestion process, the leaching residues from the 750 µm sample were ground again, digested with an acid mixture containing HF (total digestion) and the leachate was analysed. The analytical procedure for these residues is described in Hubau et al. (2019). The analysis revealed no detectable presence of the six metals considered. Therefore, it may be assumed that Cu, Fe, Pb, Zn, Ni and Co were fully leached from the 750 µm sample. Particle size regulates the surface exposed to attack by acid, and may thus significantly affect the kinetics and yield of digestion and hence the apparent metal content. More specifically, for a given mass analysed, a larger grain size will correspond to surfaces being less accessible to leaching reagents, which in turn may lead to metal dissolution and therefore a lower apparent metal content. If the 2 mm sample had affected the determination of the metal content, the mean value of the 2 mm sample would have been systematically lower than the other mean values, but this was not the case. As seen previously, there was no evident bias for the Ni, Pb, Zn, Fe, Cu and Co mean content, indicating that there is no observable relationship between the efficiency of digestion and particle sizes. It is expected that these six metals were also fully leached from the 200 µm and 2 mm sample.

3.3. Measurement deviation

For the six metals, the Relative Standard Deviation (table 2) showed two trends: i) a decrease in particle size reduces the RSD and ii) for most of the conditions, an increase in the sample mass used for digestion decreases the RSD (5 g < 2 g < 0.5 g). As expected, grinding

particles to obtain the finest sample enhanced the repeatability of the concentration measurements. This is consistent with the Gy theory of sampling (Gy, 1979). The influence of the sample mass on the RSD is also consistent with this theory, despite the results of Andrade et al. (2019), which concluded that for most metals, the RSD was lower with a lower sample mass. The concentration of the element studied also has an indirect effect: the RSD increases when the metallic content decreases (Cu and Fe < Pb and Zn < Ni and Co).

These results are consistent with the results from Wienold et al (2011) and Ernst et al (2003) for copper: the same trends and the same orders of magnitude of RSD are observed in their studies (Wienold et al., 2011; and Ernst et al., 2003). Wienold obtained the same results for the Cu content data set, with RSD < 10% for a 2 g sample mass and a particle size of 120 µm to 1.5 mm, and RSD of around 20% for a 0.1 g sample mass and particle size of 500 µm (n=9).

Since it is assumed that there are no biases due to the preparation of materials and the digestion and the analysis procedures, the observed deviation depends only on the residual heterogeneity in the sample. As expected, this sensitivity to content level is less visible for the finest particles: the RSD for 200 µm sample are below 8% except for Ni, which indicates low residual heterogeneity in the 200 µm sample. The RSD for Ni does not follow the same trend because of one erratic point [200 µm; 0.5 g]. For this condition, the erratic point had a value of 0.70 % while the mean value was 0.40% (figure 3). This point may be due to a "nugget" effect, i.e., the occurrence of one or several tiny single flakes of pure Ni in the sample that were not reduced even at 200 µm. Finer grinding might be required to ensure a more even distribution of Ni between the samples. This "nugget" effect with Ni is, to our knowledge, not described in the literature. It may be due to the composition of electronic components that include Ni as discrete particles.

3.4. Distribution discontinuity

Figure 3 gives an overview of the Zn, Ni and Co metal concentrations that were determined with our replicates: each metal concentration is represented by a black dot, the lines represent the median values and the crosses represent the mean values. Scatterplots for Cu, Pb and Fe are shown in the supplementary material since their distribution was similar to that for Zn, with almost no erratic points (one for Fe at 2 mm; 0.5 g). For the Ni and Co data sets, some values were erratic: Ni [200 µm; 0.5 g], Ni [2 mm; 2 g] and Co [2 mm; 2 g].

Most of these erratic points were observed in replicates from the coarse sample at 2 mm. For Co [2 mm; 2 g], the grades changed abruptly from 311 ppm (mean value) to 1153 ppm, the Ni [2 mm; 2 g] grades changed from 0.45% to 1.45% and the Fe [2 mm; 0.5 g] grades from 14% to 23%, 27% and 28%. The erratic points for Ni and Co came from the same digestion sample. The fine particles are more likely to be well disseminated in the shredded sample, and are responsible for a background grade of around 311 ppm for Co, 0.45% for Ni and 14% for Fe. In contrast, the presence or absence of coarse particles mainly made up of metal, such as Co, Ni or Fe, can have a strong impact on the analysis. The probability of having coarse particles of metal in a sub-sample is very low. The presence of these erratic points is very similar to the “gold nugget effect” found in assessments of gold deposits (Dominy et al., 2018). The Ni anomaly [200 µm; 0.5 g] is more problematic and shows that anomalies can exist even for the finest sample analysed for Ni. Although these erratic points do not appear often, once out of sixteen sample analyses is significant and can have a huge impact on analysis results.

No erratic points were observed for Cu, Pb and Zn. This does not mean that none can occur but that they are likely to be less present.

3.5. Modelling the confidence level

Based on the numerous analytical results obtained, a model was developed to calculate the margin of error, i.e. the confidence interval around the mean values. The statistical test was of the bootstrapping type, which relies on random sampling with replacements, as described in the Materials and Methods section. Figure 4 shows the change in the margin of error for Zn, Ni and Co content according to the number of analyses performed, the particle size and the sample mass, on a logarithmic scale. "Bootstraps" for other metals were also modelled, and are provided in the supplementary material. The aim of this calculation is to create a decision support tool to help choose the appropriate sample mass, particle size and number of repetitions needed to obtain a given margin of error in the value of the metal content.

It can be seen in figure 4 that the margins of error tend to drop with the first 4 to 5 digestions performed, before levelling off over the remaining digestion numbers in the range of 5 to 25, the latter being the upper limit considered in the bootstrapping procedure. It is thus noteworthy that performing only duplicates to determine the metal content will result in significant margins of error. Exemplifying this, the 95 % confidence interval for the mean value will represent 10 to 40 % of the mean value itself, considering the case of Zn, with a sample mass of 5 g and the three grain sizes. It is acknowledged that such uncertainties are high, and may constitute a serious source of error when calculating the yields and recoveries of metals in a WPCB recycling process. What appears obvious from figure 4 is that the most efficient way of increasing the level of confidence in analytical results is to reduce the particle size. Thus for Zn, with a particle size of 200 µm, the margin of error can drop quickly below 10% with only three measurement repetitions and a sub-sample mass of 2 g. This effect is most apparent when considering the case of Co regardless of the sample mass.

For all metals, the best preparation condition to achieve a low margin of error (< 10%) was the finest particle size of 200 µm and few repetitions (3 or 4) of 2 g sample digestion. However, to avoid the difficulty of shredding WPCBs to 200 µm, the 750 µm particle size was found to be acceptable, provided that the sample mass used for digestion was larger than 2 g.

Shapiro and Bartlett tests have proven that most of the elements presented do not follow a normal distribution. A non-parametric bootstrap method was therefore used to determine the margin of error for a combination of a particle size, a sample mass and a number of samples analysed. As the margin of error is calculated from an asymmetrical distribution, the mean value is not in the centre of the interval defined by the margin of error (figure 5, black lines): for each metal in all the preparation conditions, there is a larger gap between the mean value and the upper bound than with the lower bound. This specificity means that is not possible to predict the upper and the lower bounds for a new mean value by directly using the margin of error from the bootstrap results. However, it is possible to make the calculation from a normal distribution (figure 5, gray dotted lines), which gives half of the margin of error for the upper bound and half for the lower bound. Calculations were made to estimate the error for the lower and upper bounds by applying a normal distribution hypothesis. Table 3 presents the data calculated for a normal distribution ("bound from normal distribution hypothesis") and the comparison with the real bounds obtained with the bootstrap tool ("bootstrap data"), along with the "normal distribution error", which refers to the gap between the normal distribution hypothesis and the bootstrap data (see figure 5). Only results for a 0.5 g sample mass are presented here; those for other sample masses can be found in supplementary information.

Overall, for the upper bound, the difference never exceeds 8% (with triplicates) between the estimate and the actual data. Regarding the lower bound, most of the preparation conditions give a deviation lower than 9% if a triplicate sample is analysed. However, at 2 mm, the lower bound presents some significant differences for all metals except Cu. The lower bound is mostly underestimated in the case of the normal distribution. With a 0.5 g sample mass, the deviation reaches 17.9% for Fe, 65.4% for Co, 18.2% for Pb 23.3% for Ni and 21.1% for Zn. With 2 and 5 g sample masses, the deviation is greater than 15.5% for Co and Ni at 2 mm. Moreover, for Ni, the deviation of the lower bound is significant even with smaller particle sizes (11.6 and 14.3% for Ni at 750 µm and 200 µm respectively).

This comparison shows that reducing the particle size gives a better data fit with a normal distribution hypothesis. Thus, the margin of error calculated from bootstrap results can be used as an uncertainty around the mean value, except for the metals that present a nugget effect. Except for Ni, the error given by calculating the upper and lower limits as a normal distribution is less than 2% for 200 µm samples.

4. Conclusion

Taking subsamples from a portion of WPCBs could be time-consuming and costly. It is therefore essential to assess the effects of sample preparation on the quality of the results. This assessment allows the appropriate preparation procedure to be established according to data quality objectives.

A series of 9 preparation conditions for WPCB samples was analysed, producing a total of 159 data points per metal (Cu, Pb, Zn, Ni, Fe and Co), from which the effects of particle size, sample mass and digestion repetition were investigated. For some metals, Ni, Co and Fe, small amounts of concentrated nuggets of metal could inflate the total sampling variance.

Shredding to fine particles (< 200 µm) helped to reduce this effect for Co and Fe. For Ni, taking additional samples helped to characterize and manage this spatial heterogeneity.

This study shows that the uncertainty in the quantitative determination of metals in WPCBs and the dispersion of the values is closely dependent on the preparation of the materials (particle size and sample mass used for analysis) and on their metal content. As expected, the relative standard deviation increases when a larger particle size and a smaller sampling mass are considered, in line with Gy's sampling theory developed for ore sampling. This study quantifies these deviations when i) the particle sizes increase ii) the sample masses decrease and iii) indirectly when the content values decrease. Although this appears to be stating the obvious, our study allows the deviations to be quantified. The specific statistical processing of the data through bootstrapping allowed this quantification to be taken further and revealed that large uncertainties remain over metal concentrations if samples are not ground sufficiently finely, and if only a limited number of digestions are performed. These relatively large uncertainties, in comparison with ore, are associated with the highly heterogeneous compositions that exist in WPCBs. This study underlines the need to pay specific attention to these heterogeneities.

From statistical analysis of the data, the margin of error was predicted as a function of the sample mass, the particle size and the number of digestion repetitions. Experimenters need to consider the most reasonable balance between these three parameters, according to data quality objectives. The compromise achieved will differ from one metal to another and from one experimenter to the other, depending on their own technical limitations.

This article describes features of WPCB characterization data. Our main objective is now to deepen the data analysis. The application of Gy (Gy, 1979) sampling theory to WPCB is in progress and will be detailed in a forthcoming article.

Acknowledgments: This study was carried out under the French FOAMEX research project, funded by the French National Research Agency (ANR).

Bibliography

Andrade, D.F., Cardoso Machado, R., Arruda Bacchi, M., Pereira-Filho, E.R., 2019. Proposition of electronic waste as a reference material – part 1: sample preparation, characterization and chemometric evaluation. J. Anal. At. Spectrom. 34, 2394-2401. https://doi.org/10.1039/c9ja00283a

Arshadi, M., Mousavi, S.M., 2015. Multi-objective optimization of heavy metals bioleaching from discarded phone PCBs: simultaneous Cu and Ni recovery using Acidithiobacillus ferrooxidans. Sep. Purif. Technol. 147, 210-219. https://doi.org/10.1016/j.seppur.2015.04.020

Awasthi, A.K., Zlamparet, G.I., Zeng, Z., Li, J., 2018. Evaluating waste printed circuit boards recycling: Opportunities and challenges, a mini review. Waste Management & Research. 35, 346-356. https://doi.org/10.1177/0734242X16682607

Bachér, J., Kaartinen, T., 2017. Liberation of Printed Circuit Assembly (PCA) and dust generation in relation to mobile phone design in a size reduction process. Waste Manag. 60, 609-617. https://doi.org/10.1016/j.wasman.2016.09.037

Bizzo, W.A., Figueiredo, R.A., Andrade, V.F., 2014. Characterization of Printed Circuit Boards for Metal and Energy Recovery after Milling and Mechanical Separation. Materials. 7, 4555–4566. https://doi.org/10.3390/ma7064555

Bloodworth A., 2014. Resources: track flows to manage technology-metal supply. Nature. 505, 19-20. https://doi.org/10.1038/505019a

DIN 51701., 2006. Essais des combustibles solides - Échantillonnage et préparation des échantillons - Partie 2: Échantillonnage.

501 Dominy, S.C., O'Connor, L., Glass, H.J., Purevgerel, S., Xie, Y., 2018. Towards Representative
502 Metallurgical Sampling and Gold Recovery Testwork Programmes. Minerals. 8, 1-34.
503 https://doi.org/10.3390/min8050193

504 Ernst, T., Popp, R., Wolf, M., Van Eldik, R., 2003. Analysis of eco-relevant elements and noble
505 metals in printed wiring boards using AAS, ICP-AES and EDXRF. Anal. Bioanal. Chem. 375(6),
506 805–814. https://doi.org/10.1007/s00216-003-1802-8.

507 Ghosh, B., Ghosh, M.K., Parhi, P., Mukherjee, P.S., Mishra, B.K., 2015. Waste printed circuit
508 boards recycling: an extensive assessment of current status. J. Clean. Prod. 94, 5–19.
509 https://doi.org/10.1016/j.jclepro.2015.02.024.

510 Guo, C., Wang, H., Liang, W., Fu, J., Yi, X., 2011. Liberation characteristic and physical
511 separation of printed circuit board (PCB). Waste Management. 31, 2161-2166.
512 https://doi.org/10.1016/j.wasman.2011.05.011

513 Gy, P., 1979. Sampling of Particulate Materials, Theory and Practice. Elsevier, Amsterdam.

514 Hagelüken, C., 2006. Improving metal returns and eco-efficiency in electronics recycling - a
515 holistic approach for interface optimisation between pre-processing and integrated metals
516 smelting and refining. In: Proceedings of the 2006 IEEE, pp. 218–223.

517 Holgersson, S., Steenari, B.M., Björkman, M., Cullbrand, K., 2018. Analysis of the metal
518 content of small-size Waste Electric and Electronic Equipment (WEEE) printed circuit
519 boards—part 1: internet routers, mobile phones and smartphones. Resour. Conserv. Recycl.
520 133, 300-308. https://doi.org/10.1016/j.resconrec.2017.02.011

521 Hossain, M.S., Yahaya, A.N.A., Yacob, L.S., Rahim, M.Z.A., Yusof, N.N.M., Bachmann, R.T.,
522 2018. Selective recovery of copper from waste mobile phone printed circuit boards using

523 sulphuric acid leaching. Mater. Today Proc. 5, 21698-21702.
524 https://doi.org/10.1016/j.matpr.2018.07.021

525 Hubau, A., Chagnes, A., Minier, M., Touzé, S., Chapron, S., Guezennec, A.G., 2019. Recycling-
526 oriented methodology to sample and characterize the metal composition of waste Printed
527 Circuit Boards. Waste Management. 91, 62-71.
528 https://doi.org/10.1016/j.wasman.2019.04.041.

529 IEC 62321-2:2013., 2013. Determination of certain substances in electrotechnical products -
530 Part 2: Disassembly, disjunction and mechanical sample preparation.

531 Kaya, M., 2016. Recovery of metals and non-metals from electronic waste by physical and
532 chemical recycling processes. J. Waste Manag. 57, 64-90.
533 https://doi.org/10.1016/j.wasman.2016.08.004

534 Korf, N., Løvik, A.N., Figi, R., Schreiner, C., Kuntz, C., Martin Mählitz, P., Rösslein, M., Wäger,
535 P., Rotter V.S., 2019. Multi-element chemical analysis of printed circuit boards – challenges
536 and pitfalls. Waste Management. 92, 124-136.
537 https://doi.org/10.1016/j.wasman.2019.04.061.

538 Laubertova, M., Malindzakova, M., Trpcevska, J., Gajić, N., 2019. Assessment of sampling and
539 chemical analysis of waste printed circuit boards from WEEE : gold content determination.
540 Metallurgical and Materials Engineering. 25(2), 171-182. https://doi.org/10.30544/427.

541 Li, J-Y., Xu, X-L., Liu, W.Q., 2012. Thiourea leaching gold and silver from the printed circuit
542 boards of waste mobile phones. Waste Management. 32, 1209-1212.
543 https://doi.org/10.1590/0370-44672015680152

544 Mičková, V., Ružičková, S., Remeteiová, D., Laubertová, M., Dorková, M., 2018. Sampling and
545 digestion of waste mobile phones printed circuit boards for Cu, Pb, Ni, and Zn determination.
546 Chemical Papers. 12, 1231-1238. https://doi.org/10.1007/s11696-017-0353-y

547 Ning, C., Lin, C.S.K., Hui, D.C.W., McKay, G., 2017. Waste Printed Circuit Board (PCB)
548 Recycling Techniques. In: Lin C. (eds), Chemistry and Chemical Technologies in Waste
549 Valorization. Topics in Current Chemistry Collections. Springer, pp. 21-56. https://doi:
550 10.1007/s41061-017-0118-7

551 Ogunniyi, I.O., Vermaak, M.K.G., Groot, D.R., 2009. Chemical composition and liberation
552 characterization of printed circuit board comminution fines for beneficiation investigations.
553 Waste Manage. 29(7), 2140–2146. https://doi.org/10.1016/j.wasman.2009.03.004.

554 Otsuki, A., Pereira Gonçalves, P., Leroy, E., 2019. Selective Milling and Elemental Assay of
555 Printed Circuit Board Particles for Their Recycling Purpose. Metals. 9, 899.
556 https://doi:10.3390/met9080899

557 Otsuki, A., De la Mensbruge, L., King, A., Serranti, S., Fiore, L., Bonifazi, G., 2020. Non-
558 destructive characterization of mechanically processes waste printed circuit boards – particle
559 liberation analysis. Waste Management. 102, 510-519.
560 https://doi.org/10.1016/j.wasman.2019.11.006

561 Priya, A., Hait, S., 2018a. Extraction of metals from high grade waste printed circuit board by
562 conventional and hybrid bioleaching using Acidithiobacillus ferrooxidans. Hydrometallurgy.
563 177, 132-139. https://doi.org/10.1016/j.hydromet.2018.03.005.

564 Priya, A., Hait, S., 2018b. Comprehensive characterization of printed circuit boards of various
565 end-of-life electrical and electronic equipment for beneficiation investigation. Waste
566 Management. 75, 103–123. https://doi.org/10.1016/j.wasman.2018.02.014

567 R Core Team., 2019. R: A language and environment for statistical computing. R Foundation
568 for statistical computing. Vienna, Austria. https://www.R-project.org.

569 Rocchetti, L., Amato, A., Beolchini, F., 2018. Printed circuit board recycling: a patent review.
570 J. Clean. Prod. 178, 814–832. https://doi.org/10.1016/j.jclepro.2018.01.076.

571 UMICORE 2012. Hoboken site visit.
572 https://www.umicore.com/storage/migrate/2012SeptHobokenSiteVisitEN.pdf

573 WEB 1. http://www.urbanmineplatform.eu, last accessed on 06/25/2020

574 Wienold, J., Recknagel, S., Scharf, H., Hoppe, M., Michaelis, M., 2011. Elemental analysis of
575 printed circuit boards considering the ROHS regulations. Waste Manag. 31, 530–535.
576 https://doi.org/10.1016/j.wasman.2010.10.002.

577 Yamane, L.H., De Moraes, V.T., Espinosa, D.C.R., Tenório, J.A.S., 2011. Recycling of WEEE:
578 characterization of spent printed circuit boards from mobile phones and computers. Waste
579 Management. 31(12), 2553-2558. https://doi:10.1016/j.wasman.2011.07.006.

580 Zhao, C., Zhang, X., Ding, J., Zhu, Y., 2017. Study on recovery of valuable metals from waste
581 mobile phone PCB particles using liquid-solid fluidization technique. Chem. Eng. J. 311, 217 –
582 226. https://doi.org/10.1016/j.cej.2016.11.091

583 Zhou C., Pan Y., Lu M., Yang C., 2016. Liberation characteristics after cryogenic modification
584 and air table separation of discarded printed circuit boards. J. Haz. Mat., 311, 203-209.
585 https://doi.org/10.1016/j.jhazmat.2016.03.008

586 Figures

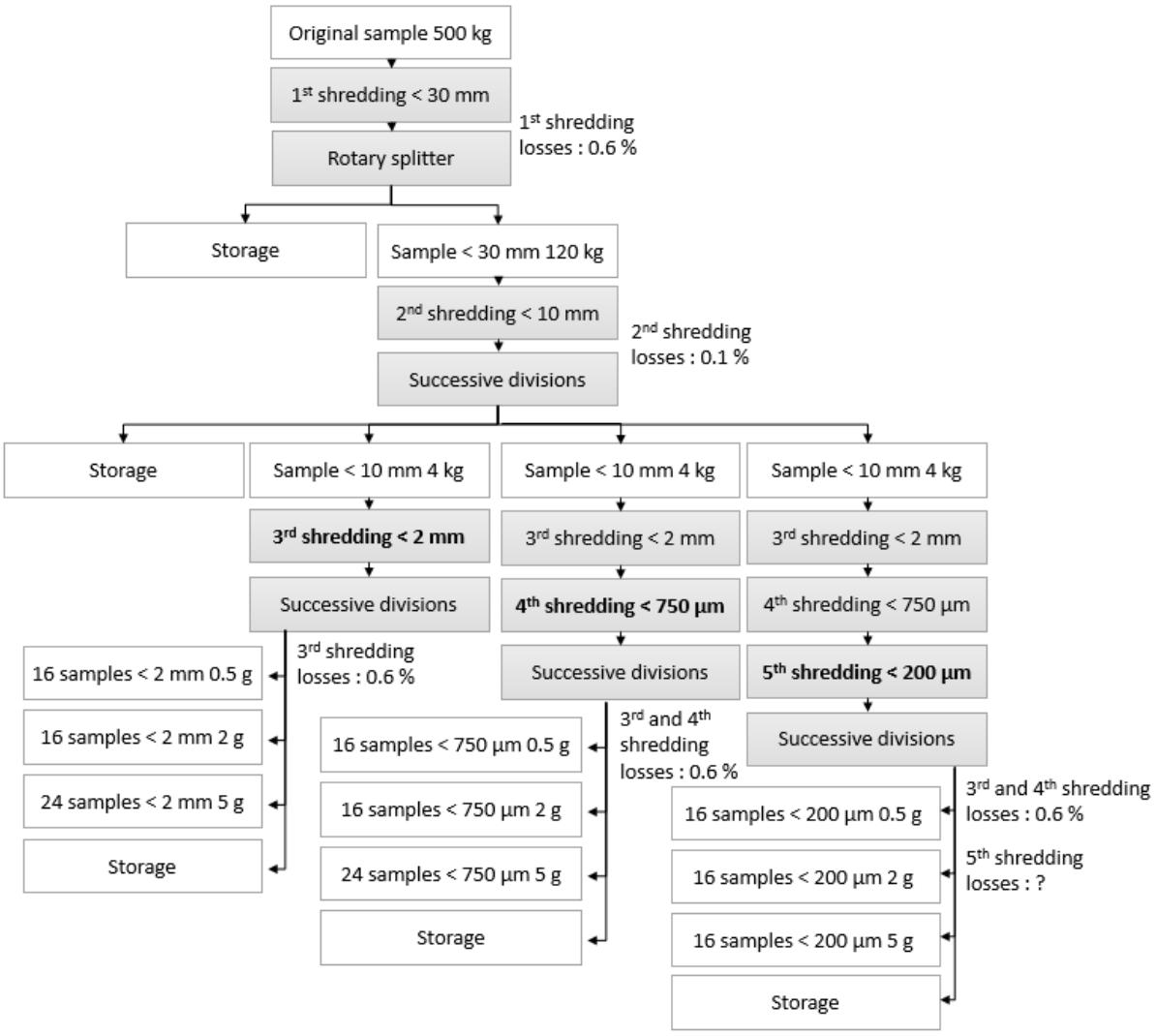

587

588 Figure 1: Sampling and shredding procedure.

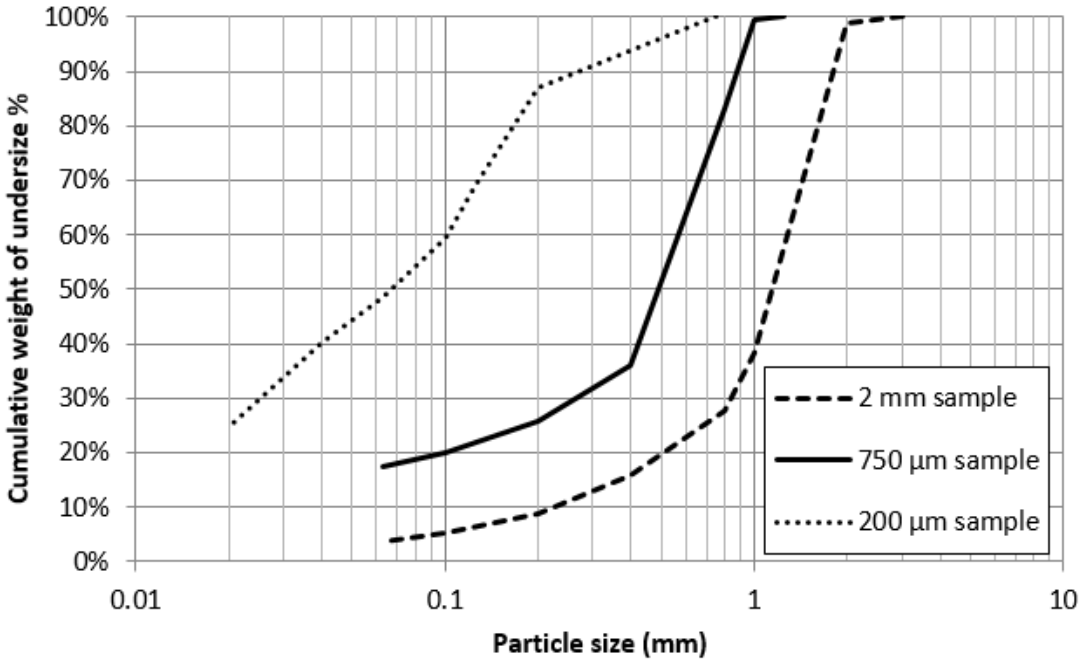

589

590 Figure 2: Particle size distributions for the 200 µm, 750 µm and 2 mm samples.

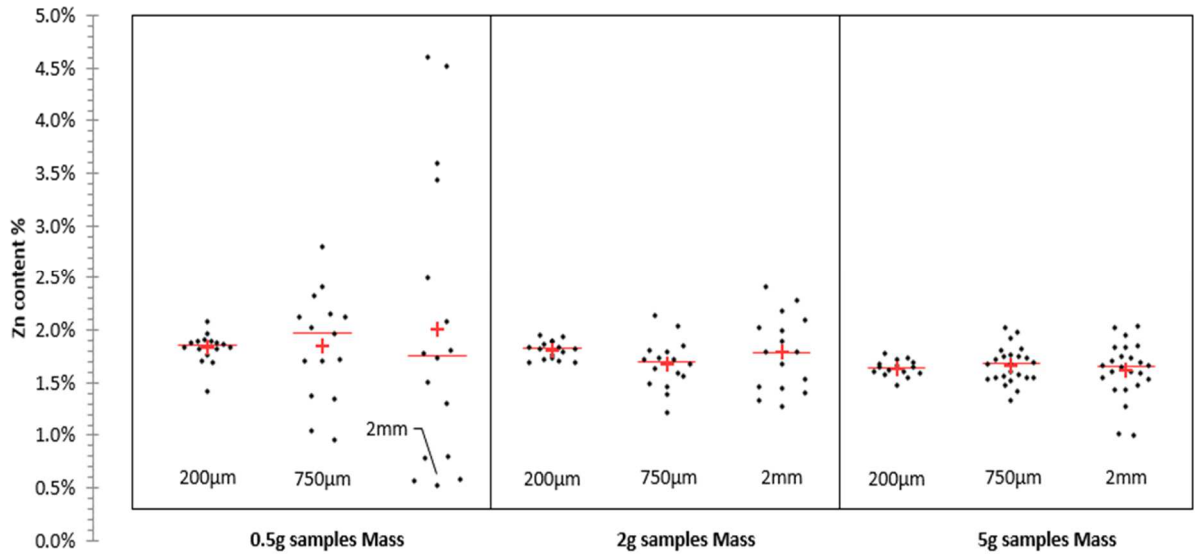
Zn content %
5.0%
4.5%
4.0%
3.5%
3.0%
2.5%
2.0%
1.5%
1.0%
0.5%
0.0%
2mm
200µm
750µm
200µm
750µm
2mm
200µm
750µm
2mm
0.5g samples Mass
2g samples Mass
5g samples Mass

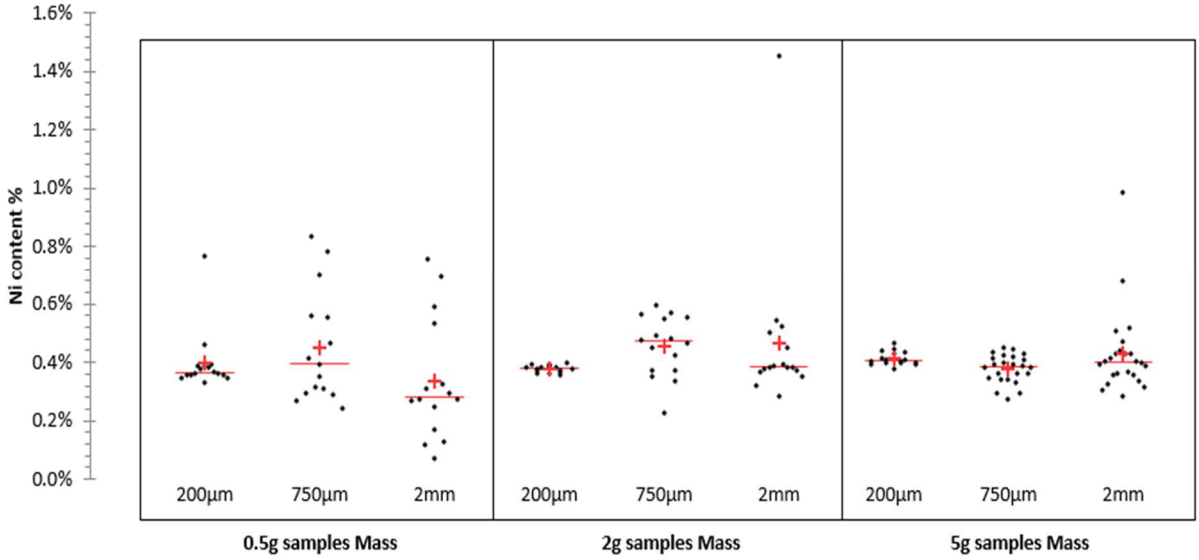
Ni content %
1.6%
1.4%
1.2%
1.0%
0.8%
0.6%
0.4%
0.2%
0.0%
200µm
750µm
2mm
200µm
750µm
2mm
200µm
750µm
2mm
0.5g samples Mass
2g samples Mass
5g samples Mass

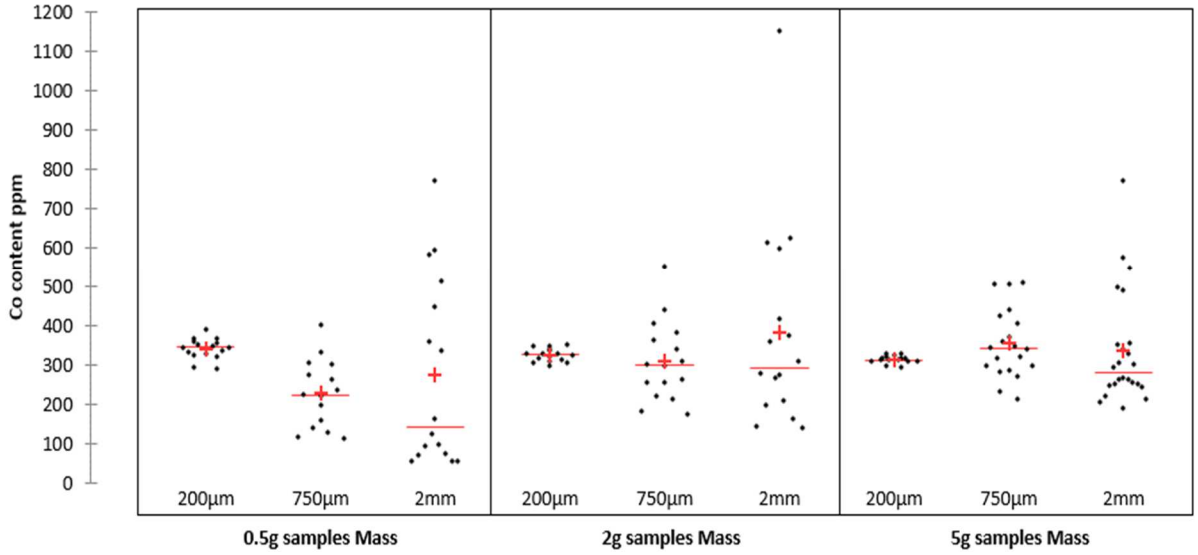
Co content ppm
1200
1100
1000
900
800
700
600
500
400
300
200
100
0
200µm
750µm
2mm
200µm
750µm
2mm
200µm
750µm
2mm
0.5g samples Mass
2g samples Mass
5g samples Mass

591

592 Figure 3: Scatterplots for Zn, Ni and Co content in WPCB according to particle size and
593 sample mass. The lines and crosses represent median and mean values respectively.

594

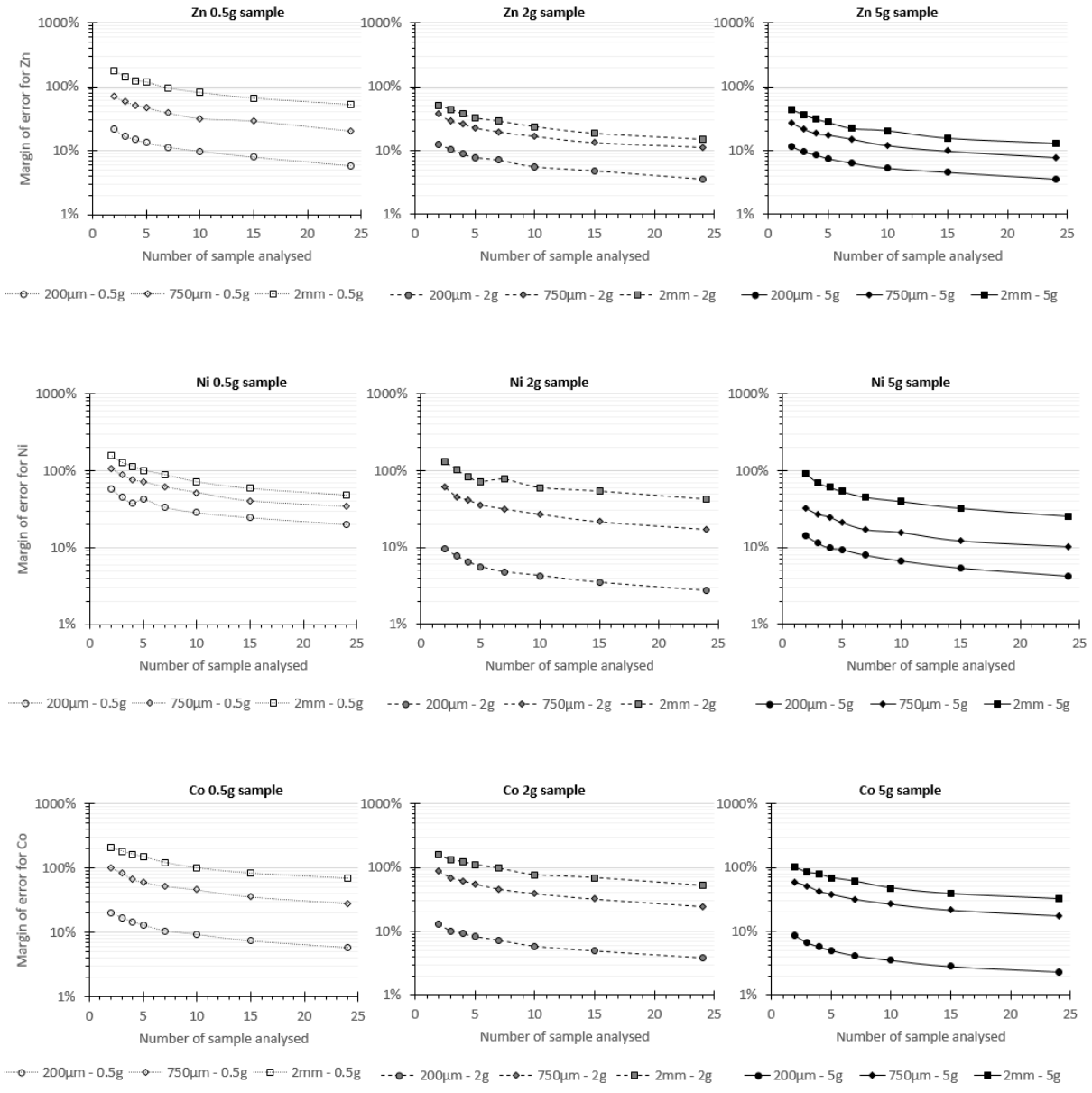

Figure 4: Margin of error for the mean values for Zn (upper figures), Ni (middle figures) and Co (lower figures) with samples of 0.5 g (left), 2 g (middle) and 5 g (right).

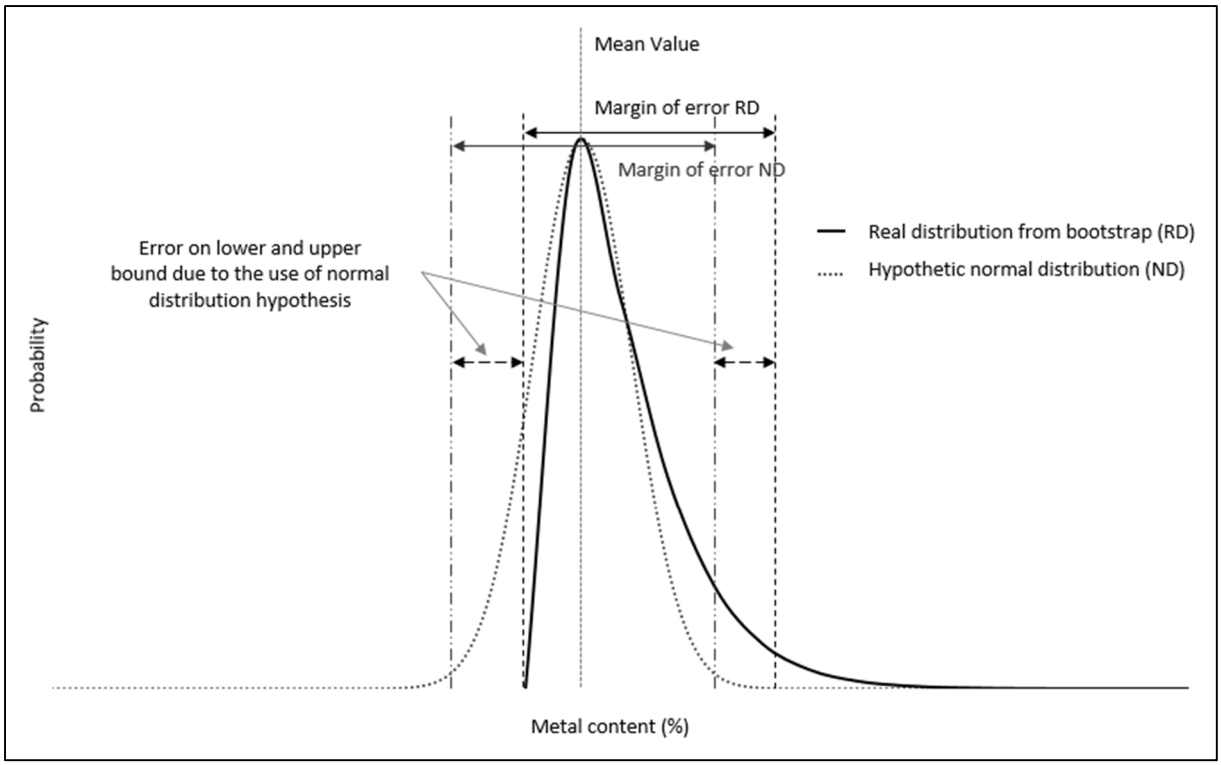

600

601 Figure 5: Comparison of the 95% confidence interval from a normal distribution and a real

602 distribution obtained by bootstrapping.

603

Tables

		0.5 g			2 g			5g		
		200 µm	750 µm	2 mm	200 µm	750 µm	2 mm	200 µm	750 µm	2 mm
Metal content	Cu %	19.6	16.4	17.2	19.1	15.8	17.2	18	15.5	16.6
	Fe %	12.8	12.2	13.6	12.6	12.2	12.3	11.9	12.2	12.3
	Pb %	1.21	1.27	1.56	1.23	1.25	1.23	1.09	1.17	1.29
	Zn %	1.83	1.85	2.01	1.81	1.67	1.79	1.64	1.67	1.62
	Ni %	0.40	0.45	0.34	0.38	0.45	0.47	0.41	0.38	0.43
	Co ppm	342	229	275	326	312	383	315	355	336

Table 1: Mean values from the nine different conditions of WPCB preparation.

Relative Standard Deviation		0.5g			2g			5g		
		200µm	**750µm**	**2mm**	**200µm**	**750µm**	**2mm**	**200µm**	**750µm**	**2mm**
	Cu	5%	9%	24%	3%	11%	11%	3%	6%	7%
	Fe	5%	18%	50%	5%	13%	14%	4%	5%	9%
	Pb	2%	28%	58%	2%	14%	22%	4%	9%	13%
	Zn	8%	28%	68%	5%	14%	20%	5%	10%	16%
	Ni	26%	43%	61%	3%	23%	58%	6%	13%	34%
	Co	8%	38%	87%	5%	33%	68%	3%	25%	42%

608

609 Table 2: Relative Standard Deviations (RSD) for the nine different conditions of WPCB

610 preparation.

	Particle size	Sample mass (g)	Mean value	Bounds from normal distribution hypothesis		*Bounds from Bootstrap data*			*Normal distribution error*	
				Lower bound	Upper bound	*Margin of error (%)*	*Lower bound*	*Upper bound*	*Lower bound*	*Upper bound*
Zn %	**200 µm**	**0.5 g**	1.83	1.68	1.99	*16.9*	*1.65*	*1.96*	1.5%	1.3%
	750 µm		1.88	1.34	2.43	*58.0*	*1.34*	*2.43*	0.4%	0.2%
	2 mm		2.00	0.56	3.44	*144*	*0.71*	*3.59*	**21.1%**	4.2%
Ni %	**200 µm**	**0.5 g**	0.40	0.31	0.49	*45.0*	*0.35*	*0.53*	**11.4%**	7.5%
	750 µm		0.45	0.25	0.65	*88.9*	*0.28*	*0.68*	**10.7%**	4.4%
	2 mm		0.33	0.12	0.55	*130*	*0.15*	*0.58*	**23.3%**	6.0%
Co ppm	**200 µm**	**0.5 g**	343	315	372	*16.6*	*312*	*369*	0.8%	0.7%
	750 µm		229	133	325	*83.8*	*131*	*323*	1.5%	0.6%
	2 mm		273	24	523	*183*	*68.0*	*567*	**65.4%**	7.8%
Cu %	**200 µm**	**0.5 g**	20	18.7	20.5	*9.2*	*18.6*	*20.4*	0.5%	0.5%
	750 µm		16.5	14.8	18.2	*20.6*	*14.5*	*17.9*	2.1%	1.7%
	2 mm		17	12.7	21.4	*51.2*	*12.8*	*21.5*	1.2%	0.7%
Fe %	**200 µm**	**0.5 g**	12.8	12.2	13.4	*9.4*	*12.2*	*13.4*	0.1%	0.1%
	750 µm		12.2	10.0	14.5	*36.9*	*10.3*	*14.8*	2.9%	2.0%
	2 mm		13.6	6.8	20.3	*99*	*8.3*	*21.8*	**17.9%**	6.9%
Pb %	**200 µm**	**0.5 g**	1.21	1.18	1.23	*4.3*	*1.18*	*1.23*	0.2%	0.2%
	750 µm		1.28	0.86	1.70	*65.2*	*0.88*	*1.71*	1.7%	0.9%
	2 mm		1.53	0.56	2.49	*126.4*	*0.69*	*2.62*	**18.2%**	4.8%

611 Table 3: Comparison between upper and lower bounds from the normal distribution hypothesis and from bootstrap data for triplicates of 0.5 g

612 sample mass and particle sizes of 200 µm, 750 µm and 2 mm.

613